Supplement to "The biggest losers: Habitat isolation deconstructs complex food webs from top to bottom"

Johanna Häussler[1,2,†,*], Remo Ryser[1,2,†], Markus Stark[3,†], Ulrich Brose[1,2], Björn C. Rall[1,2,*], and Christian Guill[3]

[1]EcoNetLab, German Centre for Integrative Biodiversity Research (iDiv) Halle-Jena-Leipzig, Deutscher Platz 5e, 04103 Leipzig, Germany

[2]Institute of Biodiversity, Friedrich Schiller University Jena, Dornburger-Strasse 159, 0773 Jena, Germany

[3]Institute of Biochemistry and Biology, University of Potsdam, Maulbeerallee 2, 14469 Potsdam, Germany

[†]These authors contributed equally

[*]Correspondence and requests should be addressed to johanna.haeussler@idiv.de and bjoern.rall@idiv.de

S1 Food web and local population dynamics

We use an allometric trophic network model (ATN model) based on the work of Schneider *et al.* [1] & Kalinkat *et al.* [2] to simulate the feeding dynamics of local populations. The topological network model is an extension of the niche model originally introduced by Williams & Martinze [3] and accounts for allometric degree distributions and recent data on scaling relationships for species body mass and trophic levels [4]. In this model framework, each species i is completely characterised by its body mass m_i, i.e. body masses determine presence/absence and strength of feeding links as well as the species' metabolic rates. The $\log_{10}$ body masses of animal species are drawn at random from the inclusive interval $(2, 12)$ and the $\log_{10}$ body masses of plant species are drawn from the inclusive interval $(0, 6)$, both with uniform probability density. This step makes the model inherently stochastic, but from hereon, all other steps are completely deterministic.

Data from empirical feeding interactions are used to parametrise the functions that characterise the optimal prey body mass and the location and width of the feeding niche of a predator. From each m_i a unimodal attack kernel, called feeding efficiency, L_{ij}, is constructed which determines the probability of consumer species i to attack and capture an encountered resource species j. We model L_{ij} as an asymmetrical hump-shaped Ricker's function (Equation T1-4) that is maximised for an energetically optimal resource body mass (optimal consumer-resource body mass ratio $R_{opt} = 100$) and has a width of $\gamma = 2$. The maximum of the feeding efficiency L_{ij} equals 1.

Table S1: Ordinary differential equations extracted from Schneider *et al.* [1] describing the local population dynamics driven by feeding interactions. We use the same allometric constraints and parameter ranges.

Equation No.	Model equations	Description
Equation T1-1	Animal population dynamics $\frac{dA_{i,z}}{dt} = e_P A_{i,z} \sum_j F_{ij,z} + e_A A_{i,z} \sum_k F_{ik,z} - \sum_k A_{k,z} F_{ki,z} - x_i A_{i,z}$	Rate of change of biomass density of animal species i on patch z; with conversion efficiency $e_P = 0.45$ typical for herbivory; conversion efficiency $e_A = 0.85$ typical for carnivory; feeding rate $F_{ij,z}$ of consumer i on resource j on patch z; metabolic demands per unit biomass for animals $x_i = x_A m_i^{-0.25}$ with scaling constant $x_A = 0.314$. The first sum goes over all plant resources j, the second over all animal resources k and the third over all animal predators k of animal species i.
Equation T1-2	Functional response $F_{ij,z} = \frac{\omega_i b_{i,j} R_{j,z}^{1+q}}{1 + c A_{i,z} + \omega_i \sum_k b_{ik} h_{ik} R_{k,z}^{1+q}} \cdot \frac{1}{m_i}$	Per unit biomass feeding rate of consumer i as function of its own biomass density, A_i, (taking interference competition c, which is the time lost due to intraspecific encounters, sampled from a normal distribution with mean $\mu_c = 0.8$ and s.d. $\sigma_c = 0.2$ for each food web), and biomass density of the resource R_j (either animal A_j or plant species P_j); with b_{ij}, resource specific capture coefficient (Eq. T1-3); h_{ij}, resource-specific handling time (Eq. T1-5); $\omega_i = 1/$(number of resource species of i), relative consumption rate accounting for the fact that a consumer has to split its consumption if it has more than one resource species.

Continued on next page

Table S1 – continued from previous page

Equation No.	Model equations	Description
Equation T1-3	Capture coefficient $b_{ij} = b_0 m_i^{\beta_i} m_j^{\beta_j} L_{ij}$	Resource specific capture coefficient of consumer species i on resource species j scaling the feeding kernel L_{ij} by a power function of consumer and resource body mass, assuming that the encounter rate between consumer and resource scales with their respective movement speed. We sample the exponents β_i and β_j from normal distributions (mean $\mu_{\beta_i} = 0.47$, s.d. $\sigma_{\beta_i} = 0.04$; $\mu_{\beta_j} = 0.15$, s.d. $\sigma_{\beta_j} = 0.03$, respectively). We assume a constant scaling factor for all capture coefficients of $b_0 = 50$. For plant resources, $m_j^{\beta_j}$ was replaced with the constant value 20 (as plants do not move).
Equation T1-4	Feeding efficiency $L_{ij} = \left(\frac{m_i}{m_j R_{opt}} e^{1 - \frac{m_i}{m_j R_{opt}}} \right)^{\gamma}$	The probability of consumer i to attack and capture an encountered resource j (which can be either plant or animal), described by an asymmetrical hump-shaped curve (Ricker's function), with width γ = 2 centered around an optimal consumer-resource body mass ratio $R_{opt} = 100$.
Equation T1-5	Handling time $h_{ij} = h_0 m_i^{\eta_i} m_j^{\eta_j}$	The time consumer i needs to kill, ingest and digest resource species j, with scaling constant $h_0 = 0.4$ and allometric exponents η_i and η_j drawn from normal distributions with means $\mu_{\eta_i} = -0.48$ and $\mu_{\eta_j} = -0.66$, and standard deviations $\sigma_{\eta_i} = 0.03$ and $\sigma_{\eta_i} = 0.02$, respectively [5].
Equation T1-6	Plant population dynamics $\frac{dP_{i,z}}{dt} = r_i G_i P_{i,z} - \sum_k A_{k,z} F_{ki,z} - x_i P_{i,z}$	Rate of change of biomass density of plant species i on patch z; with predation loss $F_{ki,z}$ summed over all consumer species k feeding on plant species i; metabolic demands per unit biomass for plants $x_i = x_P m_i^{-0.25}$ with $x_P = 0.138$; intrinsic growth rate $r_i = m_i^{-0.25}$; species specific growth factor G_i (Eq. T1-7).

Continued on next page

Table S1 – continued from previous page

Equation No.	Model equations	Description
Equation T1-7	Growth factor for plants $G_i = min\left(\frac{N_1}{K_{i,1}+N_1}, \frac{N_2}{K_{i,2}+N_2}\right)$	Species-specific growth factor of plants determined dynamically by the most limiting nutrient $l \in 1, 2$; with $K_{i,l}$, half-saturation densities determining the nutrient uptake efficiency assigned randomly for each plant species i and nutrient l (uniform distribution within $(0.1, 0.2)$). The term in the minimum operator approaches 1 for high nutrient concentrations.
Equation T1-8	Nutrient dynamics $\frac{dN_{l,z}}{dt} = D(S_l - N_l) - \nu_l \sum_{i,z} r_i G_i P_{i,z}$	Rate of change of nutrient concentration N_l of nutrient $l \in \{1, 2\}$ on patch z, with global turnover rate $D = 0.25$, determining the rate at which nutrients are refreshed; supply concentration S_l, determining the maximum nutrient level of each nutrient, l, drawn from normal distributions with mean $\mu_S = 10$ and standard deviation $\sigma_S = 2$ (provided $S_l > 0$); relative nutrient content in plant species biomass ν_l $(\nu_1 = 1, \nu_2 = 0.5)$.

S2 Generating landscapes

We generated differently fragmented landscapes, represented by random geometric graphs [6], by randomly drawing the locations of Z patches from a uniform distribution between 0 and 1 for x- and y-coordinates respectively. We created landscapes of different size by scaling the maximum dispersal distance of all organisms δ_{max} with a factor, Q, to represent landscape sizes with edge lengths between 0.01 and 10. We obtained the number of patches, Z, by using a stratified random sampling approach, i.e. we added a random number drawn from an integer uniform distribution between 0 and 9 to a series of numbers of $10, 20, \ldots, 60$. Similarly, we set the landscape size, Q, by adding a random number drawn from a uniform distribution between 0 and 1 (respectively 0 and 0.1 for landscape sizes below 1) to a series of numbers of $0.01, 0.1, 0.2, 0.3, 0.5, 0.7, 0.9, 1, 3, 5, 7, 9$.

S3 Emigration

We implemented emigration as an adaptive process depending on the net growth rate rather than the population density as the dependent variable. With this approach we could integrate the local food web dynamics into the dispersal process, i.e., dispersal depends on both intra- and interspecific interactions [7]. Similar approaches have been used by e.g. Abrams & Ruokolainen [8] and Ims & Andreassen [9]

Animal dispersal rate Assuming animals to disperse from their habitat when local conditions are poor, the rate of dispersing animal biomass increases, e.g. due to resource constraints, predation pressure or intra- and interspecific competition [10]. We thus used the net growth rate of a species on a particular patch to integrate such emigration triggers. Consequently, animal species emigrate at a higher rate when the net growth rate is low (figure S2a).

Plant dispersal rate For plants, we also assumed an additional scenario as there are examples of different life history strategies. There are for example plant species which disperse from their local habitat when they are doing well, i.e. they have a high net growth rate, as they can allocate more resources into reproduction resulting in higher seed dispersal [11]. However, there are also examples where plants reallocate resources into reproduction when they are doing poorly [12] (figure S2b) .

S4 Maximum dispersal distance

For animal species, the body mass m_i determines how fast and how far they can travel through the matrix before needing to rest and feed in a habitat patch. Thus, each animal species perceives its own dispersal network dependent on its species-specific maximum dispersal distance,

$$\delta_i = \delta_0 m_i^{\epsilon}, \tag{1}$$

where the exponent $\epsilon = 0.05$ determines the slope of the body mass scaling of δ_i. We chose a positive value for ϵ to account for a higher mobility of animals with larger body masses. The intercept $\delta_0 = 0.1256$ was chosen such that the animal species with the largest possible body mass of $m_i = 10^{12}$ had a maximum dispersal distance of $\delta_i = 0.5$. Thus, the animal species with the smallest possible body mass of $m_i = 10^2$ had a maximum dispersal distance of $\delta_i = 0.158$.

As plants disperse passively, i.e. it is the seed that disperses primarily driven by e.g. winds, there is no clear relationship between plant body mass and dispersal distance [13]. Thus, for plant species, we model a random maximum dispersal distance, δ_i, independent of body mass. We sampled δ_i for each plant species from a uniform probability density within the interval $(0, 0.5)$. Thus, the best plant disperser can potentially have the same maximum dispersal distance as the largest possible animal species.

Hence, each species forms its own dispersal network which depends on the distribution of habitat patches in the landscape and its species-specific maximum dispersal distance, δ_i. This means a species can potentially disperse between two patches n and m if the distance between the two patches is smaller than its species-specific maximum dispersal distance.

S5 Maximum trophic level

S6 Additional simulations with a constant maximum dispersal distance

We repeated all simulations with a constant maximum dispersal range for all species of $\delta_{const.} = 0.5$, i.e. all species have the same spatial network, to understand the effect of the dispersal advantage of larger animals. The results from these simulations are very similar to the results with the species-specific scaling of dispersal ranges, showing the same biomass density drop of larger animals at low mean distances (figure S3).

S7 Additional simulations of the two extreme cases

To explore the extreme cases of fragmentation in our model framework, we conducted additional simulations with emigration but no immigration on patches to represent completely isolated patches (disconnected), and landscapes with patches containing all species of the meta-food-web and neither emigration nor immigration to represent one joint landscape with no fragmentation (joint). For the disconnected scenario we simulated 6 replicates for each of the 30 food webs covering in the same stratified random way as our main simulations a gradient of patch numbers between 10 and 69 and were also initialised with a subset of species (see the methods section in the paper). For the joint scenario we simulated 20 replicates for each food web containing 3 patches.

(1) Joint scenario with no dispersal mortality $\overline{\alpha}$-diversity is on average 28.34, γ-diversity 29.64 and β-diversity 1.10.

(2) Fully isolated scenario with 100% dispersal mortality $\overline{\alpha}$-diversity is on average 4.85, γ-diversity 6.50 and β-diversity 1.09.

S8 Sensitivity analysis

We tested the effect of randomly drawn dispersal parameters (maximum dispersal rate, a, and the shape of the dispersal function, b; see the manuscript, equation 3) on mean α-, β- and γ-diversity for consumers and plants respectively. We used generalised additive mixed models (GAMM) from the mgcv package in R for all sensitivity analyses. To fit the model assumptions, we logit-transformed $\overline{\alpha}$-diversity, and log-transformed β- and γ-diversity.The emigration parameters were separately used as fixed effects and the ID of the food web (1 - 30) as random factor (with normal distribution for $\overline{\alpha}$- and β-diversity, and binomial distribution for γ-diversity). Both parameters show no strong effect in all tested cases (figure S4 - S6). Only the maximum emigration rate a of consumers shows a small negative effect on γ-diversity (figure S6). As a higher maximum emigration rate results in an overall larger loss therm due to dispersal, which fits to our general findings.

S9 Initial and post-simulation β-diversity

To see how the initialised β-diversity (see Methods) influenced the post-simulation β-diversity we performed a generalised additive mixed model (GAMM) from the mgcv package in R with the initial β-diversity as fixed effect and the post-simulation β-diversity as the response variable. Both were log-transformed to fit model assumptions. The post-simulation β-diversity and initial β-diversity were not correlated. This suggests that the initial β-diversity which is due to initialising the patches in the landscape with only a subset of species from the regional species pool does not influence the post-simulation β-diversity delectably (approximate p-value: 0.367) (figure S7).

References

[1] Schneider FD, Brose U, Rall BC, Guill C, 2016 Animal diversity and ecosystem functioning in dynamic food webs. *Nature Communications* **7**, 1–8. doi:10.1038/ncomms12718

[2] Kalinkat G, Schneider FD, Digel C, Guill C, Rall BC, Brose U, 2013 Body masses, functional responses and predator–prey stability. *Ecology Letters* **16**, 1126–1134. doi:10.1111/ele.12147

[3] Williams RJ, Martinez ND, 2000 Simple rules yield complex food webs. *Nature* **404**, 180–183. doi:10.1038/35004572

[4] Riede JO, Binzer A, Brose U, de Castro F, Curtsdotter A, Rall BC, Eklöf A, 2011 Size-based food web characteristics govern the response to species extinctions. *Basic and Applied Ecology* **12**, 581–589. doi:10.1016/J.BAAE.2011.09.006

[5] Rall BC, Brose U, Hartvig M, Kalinkat G, Schwarzmüller F, Vucic-Pestic O, Petchey OL, 2012 Universal temperature and body-mass scaling of feeding rates. *Phil. Trans. R. Soc. B* **367**, 2923–2934. doi:10.1098/rstb.2012.0242

[6] Penrose M, 2003 *Random geometric graphs*. Oxford University Press

[7] Fronhofer EA, *et al.*, 2017 Bottom-up and top-down control of dispersal across major organismal groups: a coordinated distributed experiment. *bioRxiv* doi:10.1101/213256

[8] Abrams PA, Ruokolainen L, 2011 How does adaptive consumer movement affect population dynamics in consumer–resource metacommunities with homogeneous patches? *Journal of Theoretical Biology* **277**, 99–110. doi:10.1016/j.jtbi.2011.02.019

[9] Ims RA, Andreassen HP, 2005 Density-dependent dispersal and spatial population dynamics. *Proceedings. Biological sciences* **272**, 913–8. doi:10.1098/rspb.2004.3025

[10] Bowler DE, Benton TG, 2005 Causes and consequences of animal dispersal strategies: relating individual behaviour to spatial dynamics. *Biological Reviews* **80**, 205–225. doi:10.1017/S1464793104006645

[11] Miyazaki Y, Osawa T, Waguchi Y, 2009 Resource level as a proximate factor influencing fluctuations in male flower production in Cryptomeria japonica D. Don. *Journal of Forest Research* **14**, 358–364. doi:10.1007/s10310-009-0148-2

[12] Furtado Macedo A, 2012 Abiotic Stress Responses in Plants: Metabolism to Productivity. In P Ahmad, M Prasad, eds., *Abiotic Stress Response in Plants*, 41–61. Springer, New York, NY. doi:10.1007/978-1-4614-0634-1

120 [13] Jenkins DG, *et al.*, 2007 Does size matter for dispersal distance? *Global Ecology and Biogeography* **16**, 415–425.
121 doi:10.1111/j.1466-8238.2007.00312.x

List of Figures

S1 Heatmap visualising the maximum trophic level within a food web (colour-coded; z-axis) in response to habitat isolation and habitat availability, i.e. the mean patch distance ($\overline{\tau}$, $\log_{10}$-transformed; x-axis) and the number of habitat patches (Z; y-axis). The heatmap was generated based on the statistical model predictions (see the methods section in the manuscript). The loss of species diversity driven by habitat isolation also translates into a loss of the maximum trophic level. 12

S2 Functions illustrating the dispersal rate d_i for animal (a) and plant species (b), where x_i marks the inflection point for each species i determined by the metabolic demands per unit biomass of species i (see Table S1). The colours blue and red represent different dispersal strategies and the respective colour gradients depict the parameter range of b, which determines the slope of the dispersal rate (see equation 3 in the manuscript). For the purpose of illustration, we set the maximum dispersal rate to $a = 0.1$ and for animals and plants $x_{i_A} = 0.314$ and $x_{i_P} = 0.1384$, respectively. 13

S3 Top row: Mean biomass densities of consumer (a)and plant species (b) over all food webs (B_i, $\log_{10}$-transformed; y-axis) in response to habitat isolation, i.e. the mean patch distance ($\overline{\tau}$, $\log_{10}$-transformed; x-axis). Each colour depicts the biomass density of species i averaged over all food webs: (a) colour gradient where orange represents the smallest, red the intermediate and blue the largest consumer species; (b) colour gradient where light green represents the smallest and dark green the largest plant species. Bottom row: Mean species-specific landscape connectance (ρ_i; y-axis) for consumer species (c) and plant species (d) over all food webs as a function of the mean patch distance ($\overline{\tau}$, $\log_{10}$-transformed; x-axis), using the same maximum dispersal distance for all species, $\delta_{const} = 0.5$. 14

S4 $\overline{\alpha}$-diversity (y-axes) of consumers and plants in dependence of the maximum emigration rate, a, and the shape of the emigration function, b respectively (x-axes). 15

S5 β-diversity (y-axes) of consumers and plants in dependence of the maximum emigration rate, a, and the shape of the emigration function, b respectively (x-axes). 16

S6 $\gamma-$diversity (y-axes) of consumers and plants in dependence of the maximum emigration rate, a, and the shape of the emigration function, b respectively (x-axes). 17

S7 The post-simulation β-diversity (y-axis) and the initial β-diversity (x-axis) were not correlated. 18

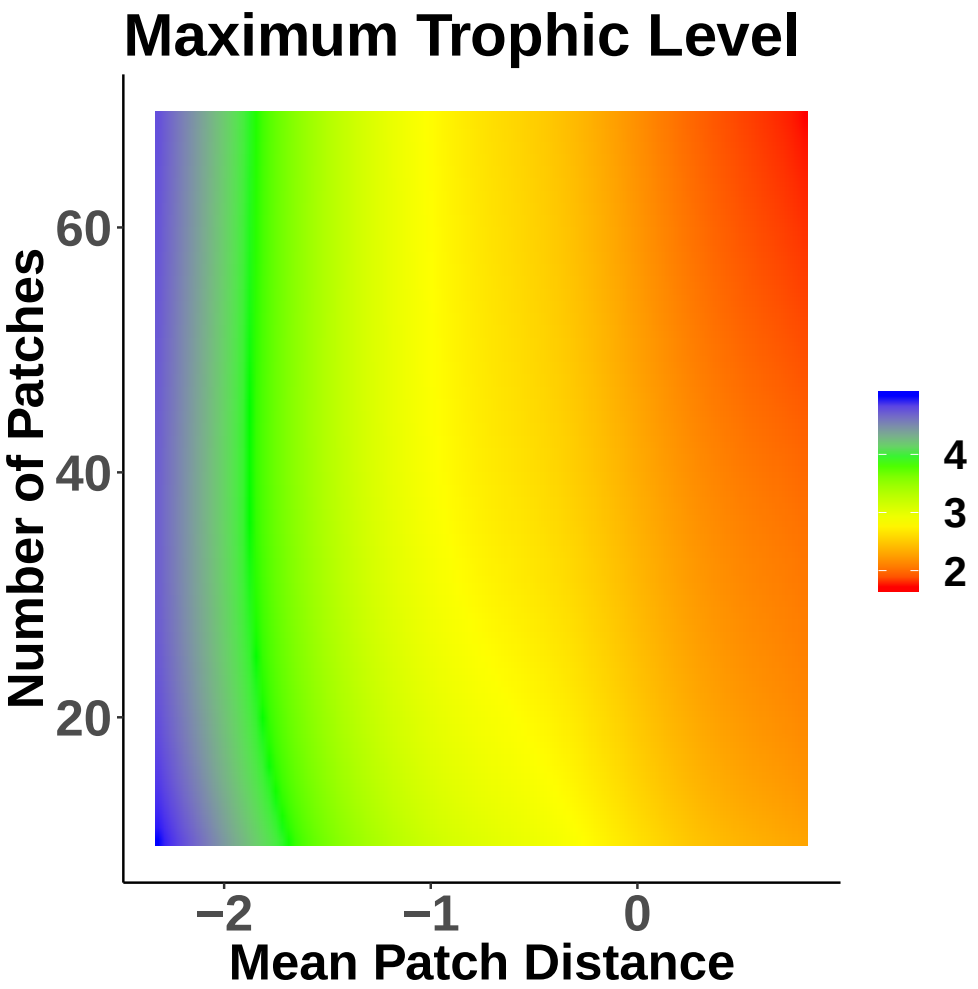

Figure S1: Heatmap visualising the maximum trophic level within a food web (colour-coded; z-axis) in response to habitat isolation and habitat availability, i.e. the mean patch distance ($\overline{\tau}$, $\log_{10}$-transformed; x-axis) and the number of habitat patches (Z; y-axis). The heatmap was generated based on the statistical model predictions (see the methods section in the manuscript). The loss of species diversity driven by habitat isolation also translates into a loss of the maximum trophic level.

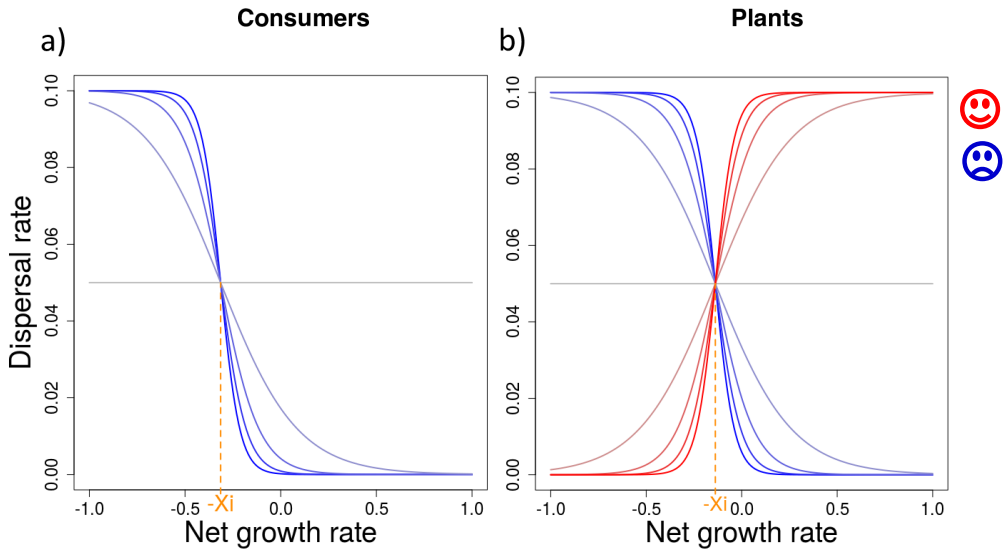

Figure S2: Functions illustrating the dispersal rate d_i for animal (a) and plant species (b), where x_i marks the inflection point for each species i determined by the metabolic demands per unit biomass of species i (see Table S1). The colours blue and red represent different dispersal strategies and the respective colour gradients depict the parameter range of b, which determines the slope of the dispersal rate (see equation 3 in the manuscript). For the purpose of illustration, we set the maximum dispersal rate to $a = 0.1$ and for animals and plants $x_{i_A} = 0.314$ and $x_{i_P} = 0.1384$, respectively.

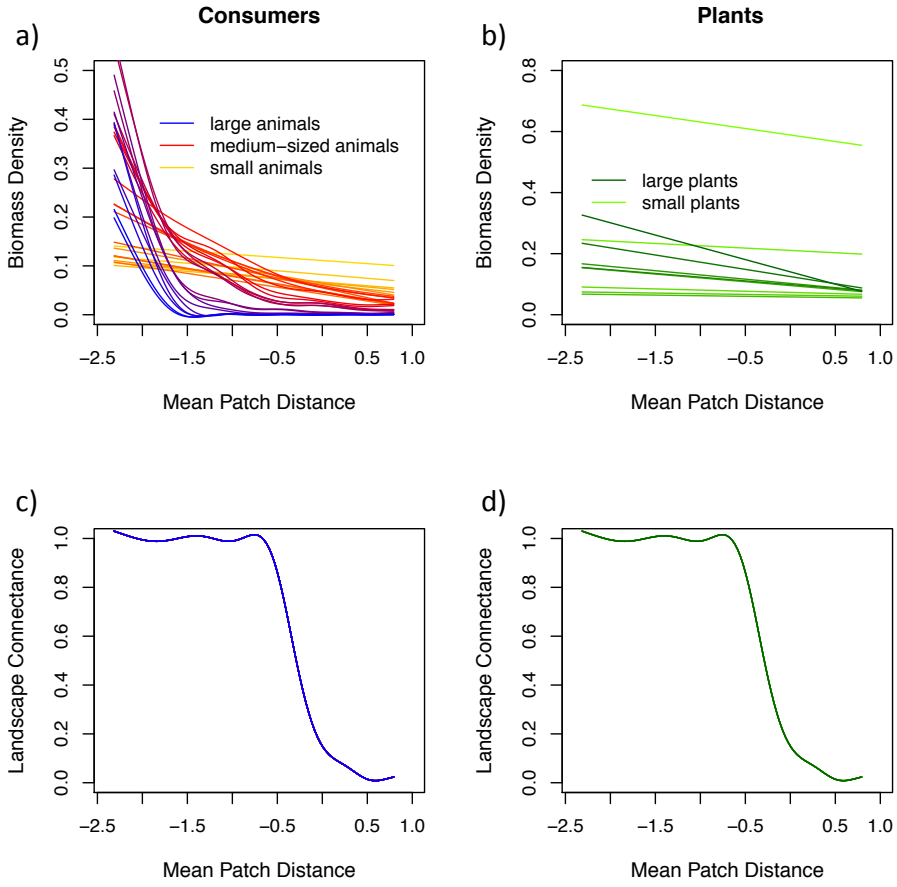

Figure S3: Top row: Mean biomass densities of consumer (a)and plant species (b) over all food webs (B_i, $\log_{10}$-transformed; y-axis) in response to habitat isolation, i.e. the mean patch distance ($\overline{\tau}$, $\log_{10}$-transformed; x-axis). Each colour depicts the biomass density of species *i* averaged over all food webs: (a) colour gradient where orange represents the smallest, red the intermediate and blue the largest consumer species; (b) colour gradient where light green represents the smallest and dark green the largest plant species. Bottom row: Mean species-specific landscape connectance (ρ_i; y-axis) for consumer species (c) and plant species (d) over all food webs as a function of the mean patch distance ($\overline{\tau}$, $\log_{10}$-transformed; x-axis), using the same maximum dispersal distance for all species, $\delta_{const} = 0.5$.

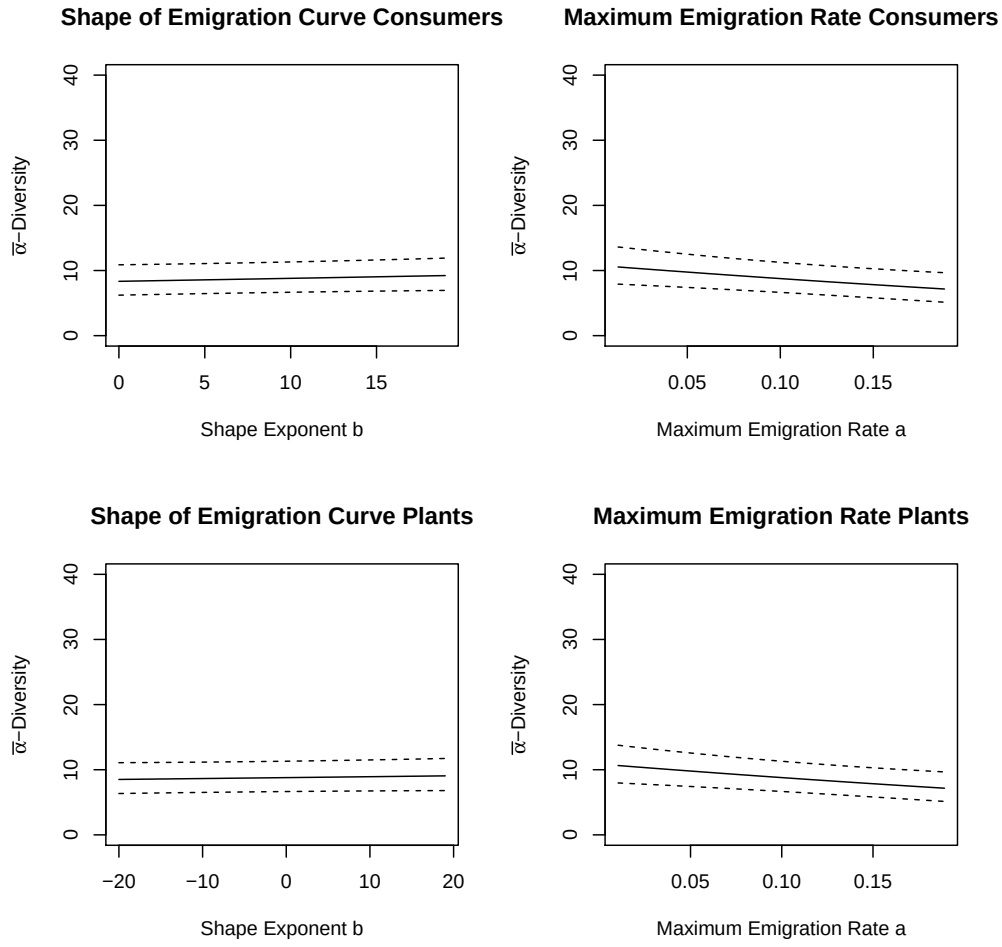

Figure S4: $\overline{\alpha}$-diversity (y-axes) of consumers and plants in dependence of the maximum emigration rate, a, and the shape of the emigration function, b respectively (x-axes).

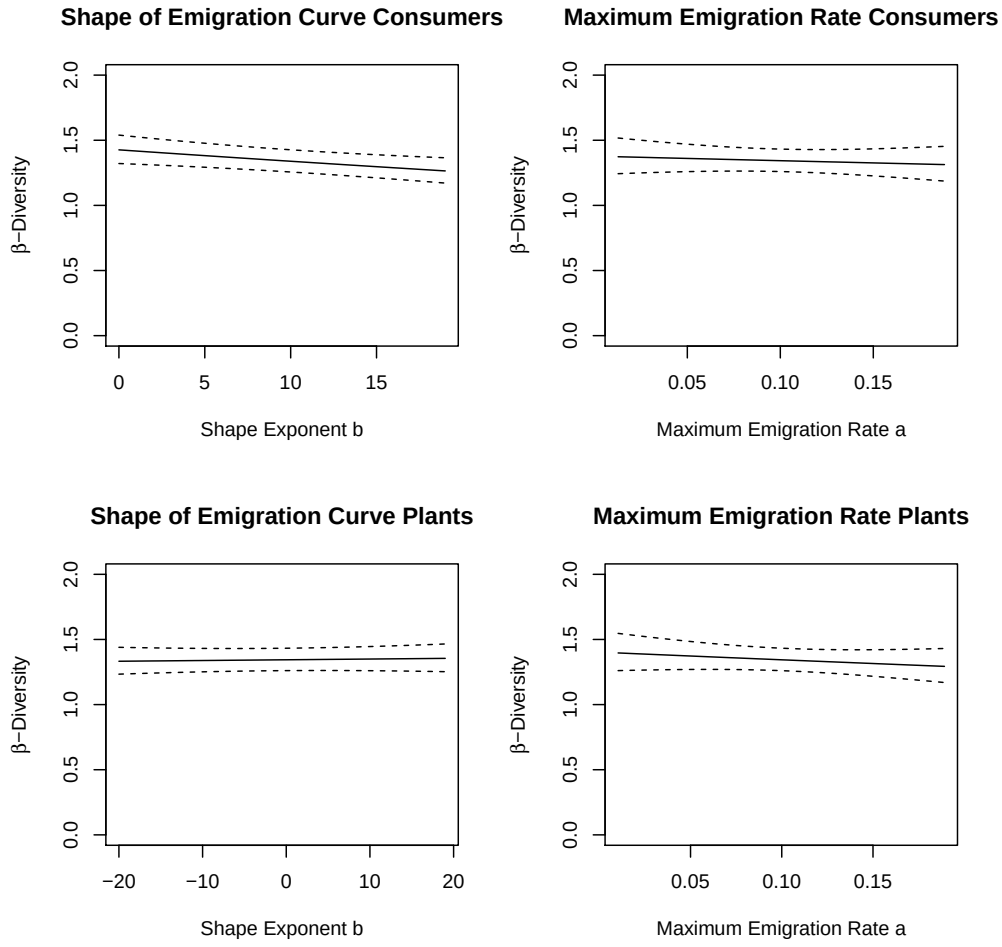

Figure S5: β-diversity (y-axes) of consumers and plants in dependence of the maximum emigration rate, a, and the shape of the emigration function, b respectively (x-axes).

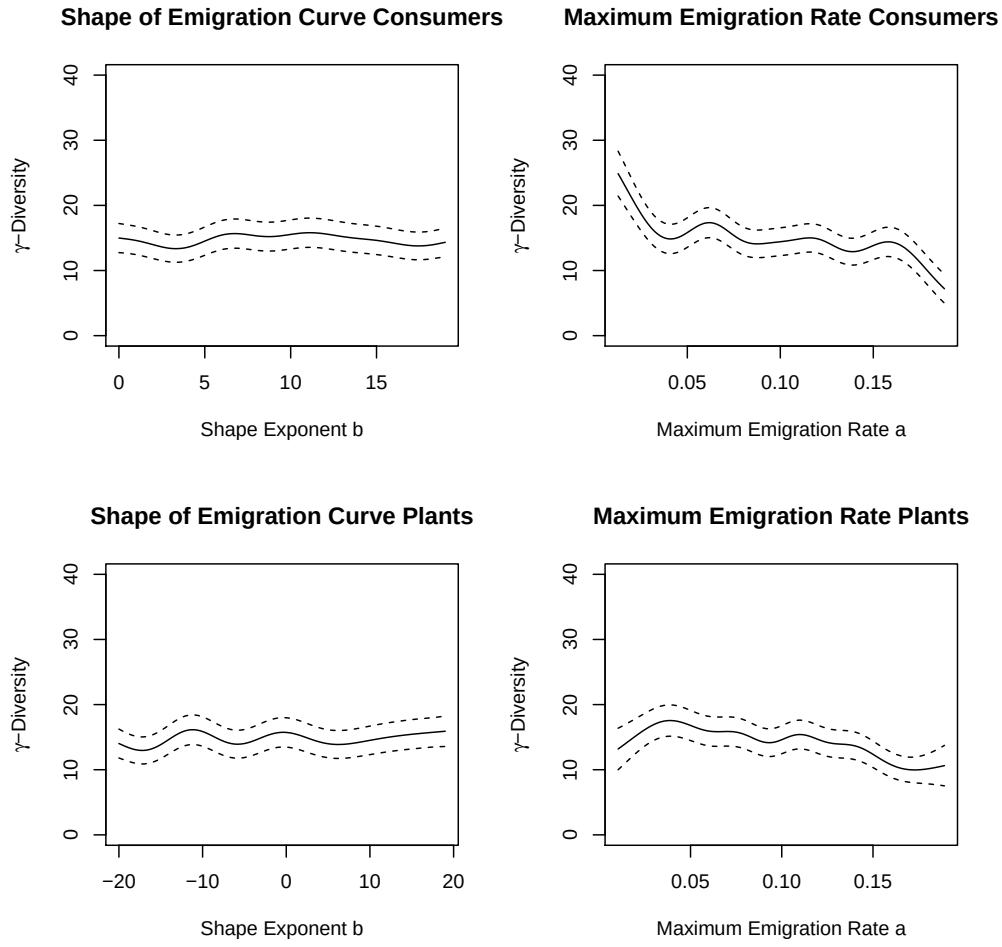

Figure S6: $\gamma-$diversity (y-axes) of consumers and plants in dependence of the maximum emigration rate, a, and the shape of the emigration function, b respectively (x-axes).

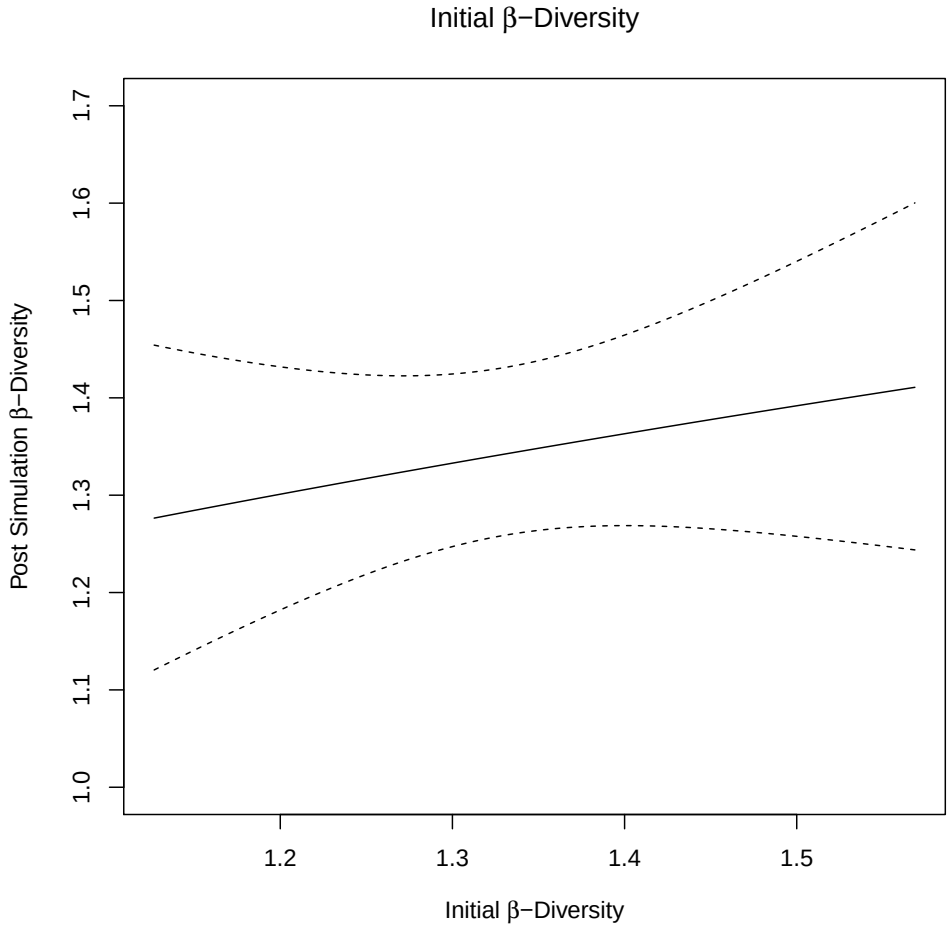

Figure S7: The post-simulation β-diversity (y-axis) and the initial β-diversity (x-axis) were not correlated.